

Surface Engineering Using Kumada Catalyst-Transfer Polycondensation (KCTP): Preparation and Structuring of Poly(3-hexylthiophene)-Based Graft Copolymer Brushes

Natalya Khanduyeva,[†] Volodymyr Senkovskyy,[†] Tetyana Beryozkina,[†] Marta Horecha,[†] Manfred Stamm,[†] Christian Uhrich,[‡] Moritz Riede,[‡] Karl Leo,[‡] and Anton Kiriy^{*†}

Leibniz-Institut für Polymerforschung Dresden e.V., Hohe Strasse 6, 01069 Dresden, Germany, and Institut für Angewandte Photophysik, Technische Universität Dresden, Helmholtzstrasse 10, 01062 Dresden, Germany

Received July 2, 2008; E-mail: kiriy@ipfdd.de

Abstract: Poly(4-vinylpyridine)-block-poly(4-iodo-styrene), P4VP-*b*-PS(I), block copolymers obtained by iodination of readily available P4VP-*b*-PS block copolymers strongly adhere to variety of polar substrates including Si wafers, glasses, or metal oxide surfaces by a polar P4VP block, forming polymer brushes of moderately stretched PS(I) chains. Kumada catalyst-transfer polycondensation (KCTP) from the P4VP-*b*-PS(I) brushes results into planar brushes of the graft copolymer in which relatively short (~10 nm) poly(3-hexylthiophene), P3HT, grafts emanate from the surface-tethered PS(I) chains. Grafting of the P3HT leads to significant stretching of the PS(I) backbone as a result of increased excluded volume interactions. Specific adsorption of the P4VP block to polar surfaces was utilized in this work to pattern the P4VP₂₅-*b*-PS(I)₃₅₀ brush. The microscopically structured P4VP₂₅-*b*-PS(I)₃₅₀ brush was converted into the respectively patterned P4VP-PS(I)-*g*-P3HT one using KCTP. We also demonstrated that KCTP from functional block copolymers is an attractive option for nanostructuring with polymer brushes. P4VP₇₅-*b*-PS(I)₃₁₃ micelles obtained in selective solvent for the PS(I) block form a quasi-ordered hexagonal array on Si wafer. The P4VP₇₅-*b*-PS(I)₃₁₃ monolayer preserves the characteristic quasi-regular arrangement of the micelles even after extensive rinsing with various solvents. Although the grafting of P3HT from the nanopatterned P4VP₇₅-*b*-PS(I)₃₁₃ brush destroys the initial order, the particulate morphology in the resulting film is preserved. We believe that the developed method to structured brushes of conductive polymers can be further exploited in novel stimuli-responsive materials, optoelectronic devices, and sensors.

Introduction

Polymers that have been terminally physisorbed or chemically grafted onto a solid surface to form polymer brushes have attracted much interest because of their importance for surface modification,¹ colloid stabilization,² for fabrication of stimuli-responsive materials,³ sensors,⁴ in microfluidics,⁵ for biomedical applications,⁶ etc. The development of this field toward always more complex and more functional materials and devices

requires both exploration of new architectures of polymer brushes and involvement of new classes of polymers into the brushlike configuration. To this end, polymer brushes that contain hydrophobic,⁷ hydrophilic,⁸ thermo-,⁹ photo-,¹⁰ and pH-responsive¹¹ polymers, as well as biorelated macromolecules¹² were already prepared and investigated. Conjugated (or conductive) polymers (CPs)¹³ is another kind of polymers that would be interesting to explore in the brushlike architecture. CPs possess very useful redox, optical, and electrical properties that make them attractive materials for “plastic” electronics, for energy conversion and storage devices.¹⁴ At the same time, some

[†] Leibniz-Institut für Polymerforschung Dresden e.V.

[‡] Universität Dresden.

- (1) *Handbook of Conducting Polymers*, 3rd ed.; Skotheim, T. A.; Reynolds, J. R., Eds.; Taylor and Francis Group, LLC: Boca Raton, FL, 2007.
- (2) Napper, D. H. *Polymeric Stabilization of Colloidal Dispersions*; Academic Press: New York, 1983.
- (3) (a) Luzinov, I.; Minko, S.; Tsukruk, V. *Prog. Polym. Sci.* **2004**, *29*, 635–698. (b) Retsos, H.; Gorodyska, G.; Kiriy, A.; Stamm, M.; Creton, C. *Langmuir* **2005**, *21*, 7722–5. (c) Retsos, H.; Senkovskyy, V.; Kiriy, A.; Stamm, M.; Feldstein, M.; Creton, C. *Adv. Mater.* **2006**, *18*, 2624–8. (d) Bocharova, V.; Kiriy, A.; Oertel, U.; Stamm, M.; Stoffelbach, F.; Detrembleur, C.; Jérôme, R. *J. Phys. Chem. B* **2006**, *110*, 14640–4.
- (4) Tokareva, I.; Minko, S.; Fendler, J. H.; Hutter, E. *J. Am. Chem. Soc.* **2004**, *126*, 15950–1.
- (5) Ionov, L.; Houbenov, N.; Sidorenko, A.; Stamm, M.; Minko, S. *Adv. Funct. Mater.* **2006**, *16*, 1153–60.

- (6) Senaratne, W.; Andruzzi, L.; Ober, C. K. *Biomacromolecules* **2005**, *6*, 2427–48.
- (7) Zhao, B.; Haasch, R. T.; MacLaren, S. *J. Am. Chem. Soc.* **2004**, *126*, 6124–34.
- (8) Barentin, C.; Muller, P.; Joanny, J. F. *Macromolecules* **1998**, *31*, 2198–2211.
- (9) Jones, D. M.; Huck, W. T. S. *Adv. Mater.* **2002**, *14*, 1130–4.
- (10) Ito, Y.; Park, Y. S. *Polym. Adv. Technol.* **2000**, *11*, 136–44.
- (11) Houbenov, N.; Minko, S.; Stamm, M. *Macromolecules* **2003**, *36*, 5897–5901.
- (12) Ito, Y.; Ochiai, Y.; Park, Y. S.; Imanishi, Y. *J. Am. Chem. Soc.* **1997**, *119*, 1619–23.
- (13) *Handbook of Conducting Polymers*, 3rd ed.; Skotheim, T. A.; Reynolds, J. R., Eds.; Taylor and Francis Group, LLC: Boca Raton, FL, 2007.

conjugated polymers retain properties inherent to traditional polymers (good mechanical properties,¹⁵ thermal stability, processability, etc.),¹³ whereas any other properties, such as self-assembly,¹⁶ water-solubility,¹⁷ thermo-,¹⁸ pH-,¹⁹ or ion-responsiveness,²⁰ or bioaffinity²¹ can be additionally developed by the attachment of appropriate substituents to the conjugated backbone. Such a combination of properties in a single material might be very helpful in designing of novel stimuli-responsive systems, chemo- and biosensors, “smart” membranes, “chemical gates”, actuators, etc.

Surface-initiated polymerization is probably the most efficient way to generate polymer brushes with high grafting densities and tunable thicknesses.²² Various chain-growth polyaddition reactions, including radical and anionic polymerization of olefins,²³ ring-opening polymerization of olefins²⁴ and polypeptides,²⁵ etc., were already adapted for preparation of brushes.²² Surface-initiated polymerizations assume generation of polymerizing species by surface-immobilized initiators and growth of polymer chains via one-by-one addition of monomers to the propagating point. Since synthesis of most conjugated polymers involves a step-growth polycondensation mechanism,¹³ the preparation of CP brushes remains problematic.²⁶

Recently McCullough et al.²⁷ and Yokozawa et al.²⁸ made an important discovery that Ni-catalyzed Kumada²⁹ polycondensation into regioregular poly(3-hexylthiophene) (P3HT) proceeds in a chain-growth manner and thus, this process, in principle, might be suitable for surface-initiated preparation of brushes. Very recently we found a way for immobilization of the Ni(PPh₃)₄ catalyst onto surface-grafted poly(4-bromosty-

rene), PS(Br)³⁰ and performed the polycondensation of 2-bromo-5-chloromagnesio-3-hexylthiophene (1) monomer into P3HT selectively from the surface avoiding the formation of the polymer in the bulk solution. According to this method, P3HT layers with the thickness exceeding 150 nm and with the conductivity in a doped state up to 2 S/cm were grown from relatively thick cross-linked PS(Br) films, whereas the grafting from rather thin PS(Br) layers was much less efficient because of well-pronounced chain-termination processes.³¹ A detailed investigation of the grafting process and the structure of the resulting composite films reveal that the grafting proceeds not only from the topmost layer of PS(Br) film, but also progresses deeply inside the PS(Br) matrix.^{31a} The process results into a kind of interpenetrated network in which relatively short (~10 nm) P3HT grafts emanate from long and cross-linked PS(Br) chains.

Block copolymers constitute an attractive option for surface-engineering because of their ability to form variety of nanoscale ordered phase-separated structures.³² However, block copolymers containing conjugated blocks³³ are less abundant compared to their nonconjugated counterparts, and their phase behavior at surfaces is not always predictable.³⁴ Herein, we demonstrate how surface structures of nonconductive block copolymers, such as poly(4-vinylpyridine)-*block*-poly(4-iodo-styrene), P4VP-*b*-PS(I), can be converted into (semi)conductive material via surface-initiated KCTP of P3HT from reactive surface-grafted block copolymers.

Experimental Section

Materials. *tert*-Butylmagnesium chloride (2.0 M solution in THF), tetrakis(triphenylphosphin)-nickel(0) (Ni(PPh₃)₄), octadecyltrichlorosilane, 3-chloropropyltrimethoxysilane, *N*-isopropylacrylamide (NiPAM), methylenbisacrylamide (MBA) hydroxyethylmethacrylate (HEMA), I₂, IO₃, methanol, nitrobenzene, acrylamide (AA), pyridine, triethyl amine (TEA), 40% HF water solution, toluene, and tetrahydrofuran (THF, stabilizer-free, anhydrous) were purchased from Aldrich and used as received without further purification. Two samples of poly(4-vinylpyridine)-*block*-polystyrene (P4VP-*b*-PS) were purchased from Polymer Source Inc.: sample I, further designated as P4VP₂₅-*b*-PS₃₅₀ ($M_{n\text{P4VP}} = 2700$ g/mol, $M_{n\text{PS}} = 36\,700$ g/mol, PDI = 1.08); sample II, further designated as P4VP₇₅-*b*-PS₃₁₃ ($M_{n\text{P4VP}} = 8000$ g/mol, $M_{n\text{PS}} = 32\,900$

- (14) Forrest, S. R. *Nature* **2004**, *428*, 911–8.
 (15) Kandre, R.; Feldman, K.; Meijer, H. E. H.; Smith, P.; Schlüter, A. D. *Angew. Chem., Int. Ed.* **2007**, *46*, 4956–9.
 (16) Brunsveld, L.; Folmer, B. J. B.; Meijer, E. W.; Sijbesma, R. P. *Chem. Rev.* **2001**, *101*, 4071–97.
 (17) Matthews, J. R.; Goldoni, F.; Schenning, A. P. H. J.; Meijer, E. W. *Chem. Commun.* **2005**, 5503–5.
 (18) Balamurugan, S. S.; Bantchev, G. B.; Yang, Y.; McCarley, R. L. *Angew. Chem., Int. Ed.* **2005**, *44*, 4872–6.
 (19) Kiriy, N.; Bocharova, V.; Kiriy, A.; Stamm, M.; Krebs, F. C.; Adler, H.-J. *Chem. Mater.* **2004**, *16*, 4765–71.
 (20) Leclerc, M. *Adv. Mater.* **1999**, *11*, 1491–8.
 (21) (a) McQuade, D. T.; Pullen, A. E.; Swager, T. M. *Chem. Rev.* **2000**, *100*, 2537–74. (b) Ho, H. A.; Dore, K.; Boissinot, M.; Bergeron, M. G.; Tanguay, R. M.; Boudreau, D.; Leclerc, M. *J. Am. Chem. Soc.* **2005**, *127*, 12673–76.
 (22) Edmondson, S.; Osborne, V. L.; Huck, W. T. S. *Chem. Soc. Rev.* **2004**, *33*, 14–22.
 (23) Matyjaszewski, K.; Davis, T., Eds. *Handbook of radical polymerization*; Wiley-Interscience: Hoboken, NJ, 2002.
 (24) (a) Ivin, K. J.; Mol, C. J. *Olefin metathesis and metathesis polymerization*; Academic Press: London, 1997. (b) Lynn, D. M.; Kanaoka, S.; Grubbs, R. H. *J. Am. Chem. Soc.* **1996**, *118*, 784–90. (c) Liu, X.; Guo, S.; Mirkin, C. A. *Angew. Chem., Int. Ed.* **2003**, *42*, 4785–89.
 (25) Merrifield, R. *Science* **1965**, *150*, 178–85.
 (26) (a) Inaoka, S.; Collard, D. M. *Langmuir* **1999**, *15*, 3752–58. (b) Nakashima, H.; Furukawa, K.; Ajito, K.; Kashimura, Y.; Torimitsu, K. *Langmuir* **2005**, *21*, 5111–15. (c) Zotti, G.; Zecchin, S.; Vercelli, B.; Berlin, A.; Grimaldi, S.; Groenendaal, L.; Bertonecello, R.; Natali, M. *Chem. Mater.* **2005**, *17*, 3681–88. (d) Hagberg, E. C.; Carter, K. R. *Polym. Preprints* **2005**, *46*, 356–7. (e) Beinhoff, M.; Appapillai, A. T.; Underwood, L. D.; Frommer, J. E.; Carter, K. R. *Langmuir* **2006**, *22*, 24114. (f) Bocharova, V.; Kiriy, A.; Vinzelberg, H.; Mönch, I.; Stamm, M. *Angew. Chem., Int. Ed.* **2005**, *44*, 6391–4.
 (27) (a) Sheina, E. E.; Liu, J.; Iovu, M. C.; Laird, D. W.; McCullough, R. D. *Macromolecules* **2004**, *37*, 3526–8. (b) Iovu, M. C.; Sheina, E. E.; Gil, R. R.; McCullough, R. D. *Macromolecules* **2005**, *38*, 8649–56.
 (28) (a) Yokoyama, A.; Miyakoshi, R.; Yokozawa, T. *Macromolecules* **2004**, *37*, 1169–71. (b) Miyakoshi, R.; Yokoyama, A.; Yokozawa, T. *J. Am. Chem. Soc.* **2005**, *127*, 17542–7.
 (29) Kiso, Y.; Yamamoto, K.; Tamao, K.; Kumada, M. *J. Am. Chem. Soc.* **1972**, *94*, 4373–4.

- (30) Senkovskyy, V.; Khanduyeva, N.; Komber, H.; Oertel, U.; Stamm, M.; Kuckling, D.; Kiriy, A. *J. Am. Chem. Soc.* **2007**, *129*, 6626–32.
 (31) (a) Khanduyeva, N.; Senkovskyy, V.; Beryozkina, T.; Simon, F.; Nitschke, M.; Stamm, M.; Grötzschel, R.; Kiriy, A. *Macromolecules* **2008**, *41*, 7383–7389. (b) Beryozkina, T.; Senkovskyy, V.; Kaul, E.; Kiriy, A. *Macromolecules* **2008**, *41*, 7817–23.
 (32) Harrison, C.; Dagata, J. A.; Adamson, D. H. In *Developments in Block Copolymer Science and Technology*; Hamley, I. W., Ed.; John Wiley and Sons: New York, 2004.
 (33) (a) Scherf, U.; Gutacker, A.; Koenen, N. *Acc. Chem. Res.* **2008**, *41*, 1086–1097. (b) Liu, J.; Sheina, E.; Kowalewski, T.; McCullough, R. *Angew. Chem.* **2002**, *114*, 339–42. (c) Dai, C.-A.; Yen, W.-C.; Lee, Y.-H.; Ho, C.-C.; Su, W.-F. *J. Am. Chem. Soc.* **2007**, *129*, 11036–38. (d) Economopoulos, S. P.; Chocho, C. L.; Gregoriou, V. G.; Kallitsis, J. K.; Barrau, S.; Hadziioannou, G. *Macromolecules* **2007**, *40*, 921–7.
 (34) (a) Wang, H. B.; Wang, H. H.; Urban, V. S.; Littrell, K. C.; Thiyagarajan, P.; Yu, L. P. *J. Am. Chem. Soc.* **2000**, *122*, 6855–61. (b) Leclerc, P.; Hennebicq, E.; Calderone, A.; Brocorens, P.; Grimsdale, A. C.; Mullen, K.; Bredas, J. L.; Lazzaroni, R. *Prog. Polym. Sci.* **2003**, *28*, 55. (c) Hempenius, M. A.; Langeveld-Voss, B. M. W.; van Haare, J.; Janssen, R. A. J.; Sheiko, S. S.; Spatz, J. P.; Moller, M.; Meijer, E. W. *J. Am. Chem. Soc.* **1998**, *120*, 2798–9. (d) Surin, M.; Marsitzky, D.; Grimsdale, A. C.; Mullen, K.; Lazzaroni, R.; Leclerc, P. *Adv. Funct. Mater.* **2004**, *14*, 708–15. (e) Tao, Y.; Zohar, H.; Olsen, B. D.; Segalman, R. A. *Nano Lett.* **2007**, *7*, 2742–46.

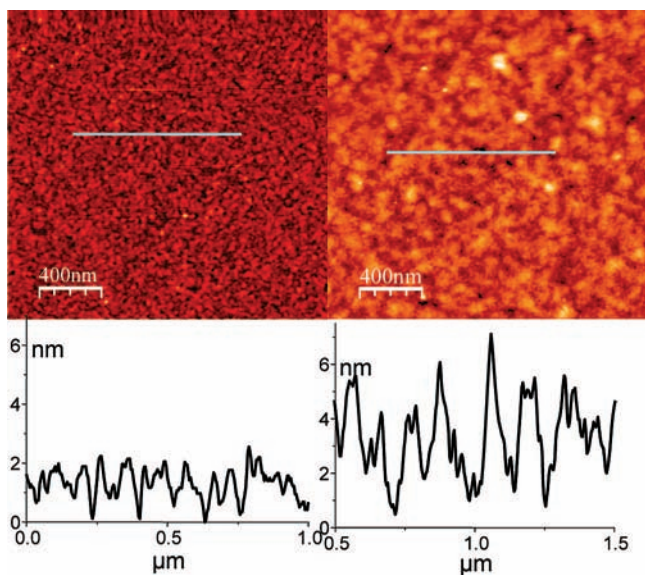


Figure 1. AFM topography images (a, b) and cross-sections (c, d) of P4VP₂₅-*b*-PS(I)₃₅₀ (a, c) and P4VP₂₅-*b*-PS(I)₃₅₀-*graft*-P3HT (b, d) brushes.

g/mol, PDI = 1.06). 2-Bromo-3-hexyl-5-iodothiophene and 2-bromo-5-chloromagnesium-3-hexylthiophene (**1**) were prepared as previously described.²⁸

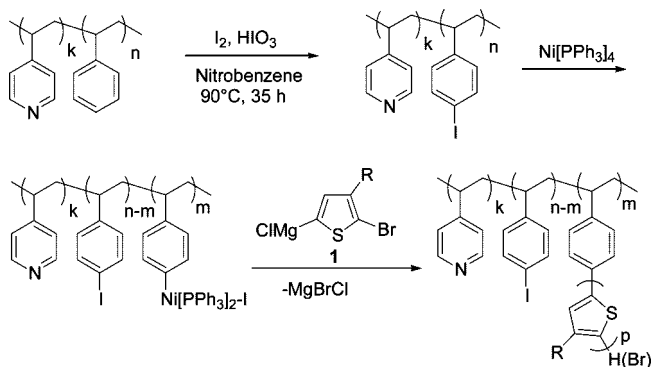
Iodination³⁵ of P4VP-*b*-PS. In a 25 mL one-necked round-bottomed flask equipped with a magnetic stir bar and reflux condenser 0.56 g of P4VP₂₅-*b*-PS₃₅₀ or 0.65 g of P4VP₇₅-*b*-PS₃₁₃ (0.005 mol of styrene monomer units) were dissolved in 15 mL of nitrobenzene and then 0.51 g (0.002 mol) of iodine, 0.19 g (0.001 mol) of iodic acid and 1 mL ~66% solution of H₂SO₄ were added and the mixture was heated at 90 °C for 35 h. Afterward, the mixture was poured into 200 mL of methanol and white precipitate was collected by filtration, washed with 10 mL of 10% NaHSO₃ solution, copious amounts of water, methanol and finally dried in vacuum at 60 °C to give ~1.0 g (>80%) of pale yellow solid of iodinated products designated as P4VP₂₅-*b*-PS(I)₃₅₀ and P4VP₇₅-*b*-PS(I)₃₁₃ (for ¹H NMR see Figure S1, Supporting Information).

Grafting of P3HT. Highly polished Si wafers (Wacker-Chemitronics), glass slides (Menzel-Glaser), or ITO glasses (Thin Film Devices) were first cleaned in an ultrasonic bath three times for 5 min with dichloromethane, placed in cleaning solution (prepared from NH₄OH and H₂O₂) for 1 h and finally rinsed several times with Millipore water (18 MQxcm).

Unstructured Films. To prepare homogeneous films, P4VP₂₅-*b*-PS(I)₃₅₀ was deposited by spin-coating from chloroform (1 mg/mL, 2000 rpm) onto Si wafers or glass slides, and the samples were annealed at 150 °C during 10 h in argon atmosphere. An excess of P4VP₂₅-*b*-PS(I)₃₅₀ was washed away by chloroform giving smooth featureless surface with a root-mean-square roughness rms ≈ 0.3 nm (Figure 1a). The typical thickness for the grafted P4VP₂₅-*b*-PS(I)₃₅₀ films is about 6–8 nm (ellipsometry). Although the grafting is provided by physisorption of the P4VP block, the films were found to be reasonably stable.

Prior to the grafting of P3HT, the samples were extensively rinsed with THF, dried, and placed into round-bottomed flask equipped with a septum, and the atmosphere was replaced by argon. Afterward, a solution of Ni(PPh₃)₄ in dry toluene (0.05 wt %, 10 mL) was added to the flask via a syringe, the samples were allowed to react overnight at room temperature. The samples were then repeatedly washed in the glovebox with dry and deoxygenated THF to remove the excess of unreacted Ni(PPh₃)₄. To this end, the reaction mixture was removed by the syringe and the new portion

Scheme 1. Iodination of P4VP-*b*-PS and Preparation of Grafted P4VP-*b*-PS(I)-*g*-P3HT via KCTP

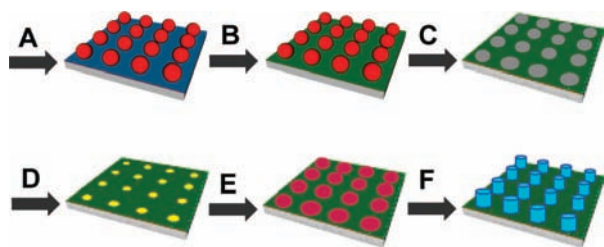


of THF was added to the flask to fully cover the samples, stirred for few minutes, and then removed. Finally, the 15 mmol/L solution of the monomer **1** in dry THF was added and the samples were allowed to polymerize at 0 °C overnight to achieve a maximal thickness of grafted P3HT (Scheme 1). The resulting composite films were found to be very robust against delamination and upon extensive rinsing with various organic solvents in ultrasonic bath and Soxhlet apparatus. AFM reveals a quite smooth morphology for P4VP-*b*-PS(I)-*g*-P3HT films with rms roughness of 1 nm (Figure 1b).

Experiments with P4VP₂₅-*b*-PS(I)₃₅₀ Immobilized onto Silica Particles. To shed a light on a cross-linking process possibly occurring at the stage of the immobilization of Ni(PPh₃)₄ catalyst, a direct analysis of polymeric materials detached from the surface is desired. For these experiments we utilized 70–230 mesh silica gel particles for chromatography (Aldrich), which were dried in vacuum overnight at 100 °C and then extensively rinsed with anhydrous THF prior usage. P4VP₂₅-*b*-PS(I)₃₅₀ (200 mg) was dissolved in 20 mL of THF, and this solution was combined with the dispersion of 7 g of silica gel in 10 mL of THF and stirred overnight. Afterward, the solvent was removed in vacuum, and the mixture of P4VP₂₅-*b*-PS(I)₃₅₀ and silica gel was annealed during 1 h at 100 °C. An excess of unattached polymer was washed away with THF and dried in a vacuum overnight at 100 °C. The content of P4VP₂₅-*b*-PS(I)₃₅₀ in the resulting composite was ~22 mg/g.

Further experiments with P4VP₂₅-*b*-PS(I)₃₅₀/silica gel composite and Ni(PPh₃)₄ were performed in a glovebox under argon atmosphere. In a typical experiment, 1 g of the P4VP₂₅-*b*-PS(I)₃₅₀/silica gel composite was dispersed in 10 mL of dry degassed toluene in round-bottomed flask equipped with a septum. Afterward, a respective amount of Ni(PPh₃)₄ solution in dry toluene was added to the flask via a syringe and the samples were allowed to react overnight at room temperature. The samples were then removed from the glovebox, and the reaction was stopped by the addition of a few drops of 5 M HCl. The solid was separated from THF solution by a vacuum filtration.

The polymer was detached from the solid support either by a treatment with pyridine/triethyl amine (TEA) mixture, or by dissolution of silica gel in HF. It was possible to isolate polymeric products from the samples prepared at Ni(PPh₃)₄-to-iodostyrene, [Ni]/S(I), ratios lower than 1:20 without complete dissolution of silica gel. In these cases, the polymer composites were dispersed in the chloroform solution of pyridine (10%, v) and TEA (1%, v) and the silica particles were separated from the solution by vacuum filtration. The detached polymers were isolated by removing of solvents in vacuum and rinsed with 25% ammonia solution, water and methanol. Finally, the polymer samples were dried (typical yield 15–18 mg) and subjected to GPC analysis. At [Ni]/S(I) ratios higher than 1:20 the pyridine/TEA treatment failed to recover the polymeric materials. Alternative detachment procedure implied dissolution of silica gel in HF (40% in water, 10 mL) and collection of the resulting insoluble material by centrifugation. The resulting solids

Scheme 2. Schematic Representation of the Micropatterning Procedure

were treated with 25% ammonia solution for deprotonation of P4VP, however even after this treatment the resulting solids obtained at [Ni]/S(I) ratios higher than 1:20 were not soluble in any solvents tried.

Grafting of P3HT from P4VP₂₅-*b*-PS(I)₃₅₀ Immobilized onto Silica Particles. Silica gel/P4VP₂₅-*b*-PS(I)₃₅₀ composite (1 g) was treated with Ni(PPh₃)₄ (using the [Ni]/S(I) ratio of ~0.8:1) in the argon glovebox, as described above. A solution (15 mmol/L) of the monomer **1** in dry THF was added and the sample was stirred at 0 °C during 3 h. After the polymerization, the resulting brown suspension was quenched with acid water, washed with copious amounts of water and methanol, redispersed in chloroform, and centrifugated. The procedure of rinsing with chloroform was repeated until a supernatant solution was virtually colorless. The resulting modified particles were treated with the 1:1 v/v mixture of 40% HF and THF at room temperature for 5 days. The insoluble material was washed with water, 25% ammonia solution in water and methanol. The residual solid (of a dark-brown color in its dry state and an orange in chloroform) was insoluble in any solvents usually suitable for the dissolution of P3HT (e.g., chloroform, xylene, chlorobenzene) even at prolonged heating. This experiment indicates that the extensive cross-linking occurs during the grafting of P3HT.

Microstructured Films. P4VP₂₅-*b*-PS(I)₃₅₀ microstructures were prepared by a kind of colloidal lithography (Scheme 2). Hydrogel particles were prepared by a precipitation-polymerization of NIPAM in the presence of MBA cross-linker³⁶ and used as a mask.

The particles were arranged on Si wafers by dip coating (step A in Scheme 2). Afterward, the samples were treated by ODS (0.4% solution in toluene) to hydrophobize the surface between the particle (step B). In the next step (C), the particles were removed by ultrasonication at 50–60 °C in the acetone/water mixture for 15 min and dried revealing micrometer-sized dots of naked Si. Then the chloroform solution of P4VP₂₅-*b*-PS(I)₃₅₀ was spin-coated and the samples were annealing at 130 °C in vacuum overnight providing the grafting of the P4VP block (step D). Finally, the samples were activated by Ni(PPh₃)₄ (step E) and P3HT was grown using KCTP using the procedure described above (step F). Each step of the micropatterning was monitored by ellipsometry and AFM.

Nanostructured Films. To prepare a micellar dispersion, P4VP₇₅-*b*-PS(I)₃₁₃ was dissolved in hot toluene (1 g/L) and allowed to equilibrate at room temperature for at least for 1 week. Afterward, the micelles were arranged by spin-coating (2000 rpm) and the samples were annealed at 150 °C during 10 h under argon. The samples were extensively rinsed with chloroform and further investigated by AFM and ellipsometry. Finally, P3HT was “grafted-on”, as described above.

Dry State Ellipsometry Thickness Measurements. The thickness of polymer layers in the dry state was measured by an SE400 ellipsometer (SENTECH Instruments GmbH, Germany) with a 632.8 nm laser at a 70° incident angle. A multilayer model has been used for calculation of the thickness of multicomponent

polymer films from the ellipsometric angles Ψ and Δ . Initially, the thickness of the native SiO₂ layer was calculated at refractive indices $n = 3.858 - i \times 0.018$ and $n = 1.4598$ for the Si wafer and the SiO₂ layer, respectively. The average thickness of the P4VP-*b*-PS(I) layer was evaluated using the two-layer model Si/SiO₂/P4VP-*b*-PS(I) with $n = 1.6$ for P4VP-*b*-PS(I). The average thickness of the grafted P3HT layer was evaluated using a three-layer model, Si/SiO₂/P4VP-*b*-PS(I)/P3HT with $n = 1.99$ for P3HT. The measurements were averaged for at least 10 points for each sample.

Swellability Experiments. In order to examine the swelling behavior of the polymer layers in THF and toluene, the measurements were carried out using null-ellipsometer in a polarizer-compensator-sample analyzer (Multiscope, Optrel Berlin) mode. As light source a He–Ne laser with $\lambda = 632.8$ nm was applied and the angle of incidence was set to 70°. An ellipsometric cell with thin glass walls, fixed at a known angle (68°) from the sample plane, was used. The angle of incidence of the light was set such that its path was normal to the window. The bilayer model (silicon/silicon oxide/swollen polymer film) was used to calculate the thickness of the swollen layer from the ellipsometric angles.³⁷

Results and Discussion

Postpolymerization modification of polymers has proven to be a general route to materials that might otherwise be difficult or impossible to make by direct polymerization routes.³⁸ Styrene, in contrast to its halogenated counterparts, can be easily polymerized by means of various controlled polymerization techniques that makes polystyrene-based block copolymers to be one of the most readily available class of well-defined polymer materials.³⁹ It was earlier found that bromine or iodine atoms can be introduced into the para position of the aromatic ring by the direct halogenation of the polystyrene homopolymer.³⁵ We found that these procedures work well also for the halogenation of P4VP-*b*-PS block copolymers, if PS is a major block.⁴⁰ For example, the iodination of P4VP₂₅-*b*-PS₃₅₀ and P4VP₇₅-*b*-PS₃₁₃ into P4VP₂₅-*b*-PS(I)₃₅₀ and P4VP₇₅-*b*-PS(I)₃₁₃, respectively, proceeds selectively into the PS-block and near quantitatively (more than 95% by NMR, Scheme 1 and Figure S1⁴¹). Although both P4VP-*b*-PS(Br) and P4VP-*b*-PS(I) can be used for further grafting of P3HT, the immobilization of the Ni catalyst proceeds much faster with PS(I), and therefore, only iodinated block copolymers were used in the present work.

Very strong, quasi-irreversible binding of polyvinyl homopolymers to various substrates was previously described.⁴² The interaction on an individual pyridyl group with the surface is not strong and can be described in terms of physisorption, however, the fact that one polymer molecule simultaneously interacts with the surface through many pyridyl groups provides an entropic advantage for the quasi-irreversible adsorption of this molecule to the surface even in the presence of strong solvents. We exploited this binding activity for the grafting of both highly asymmetric P4VP₂₅-*b*-PS(I)₃₅₀ (Figure 1a) and less asymmetric P4VP₇₅-*b*-PS(I)₃₁₃ block copolymers to Si wafers, glass slides, or ITO-coated glasses. In contrast to polymer

(37) Azzam, R. M. A.; Bashara, N. M. *Ellipsometry and Polarized Light*; North Holland: Amsterdam, 1999.

(38) Odian, G. *Principles of Polymerization*, 4th ed.; Wiley: Hoboken, NJ, 2004.

(39) Scheirs, J.; Priddy, D. *Modern styrenic polymers*; Wiley and Sons: New York, 2003.

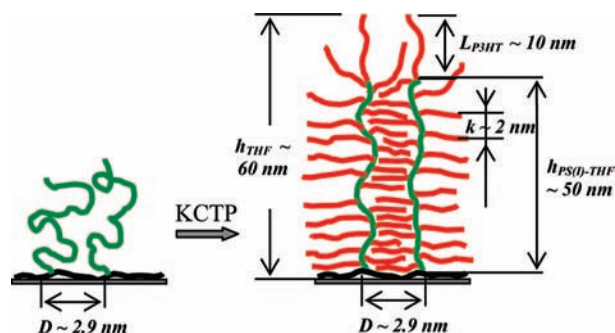
(40) Poor solubility of the P4VP block in the protonated state causes difficulties upon the iodination of P4VP-*b*-PS with high P4VP content (<50%).

(41) See Supporting information.

(42) See, for example Malynych, S.; Luzinov, I.; Chumanov, G. *J. Phys. Chem. B* **2002**, *106*, 1280–5.

(36) Zha, L.; Hu, J.; Wang, C.; Fu, S.; Ellaisari, A.; Zhang, Y. *Colloid Polym. Sci.* **2002**, *280*, 1–6.

Scheme 3. Schematic Representation of Adsorbed P4VP₂₅-*b*-PS(I)₃₅₀ Block Copolymer and P4VP-*b*-PS(I)-*g*-P3HT Brush



brushes formed upon adsorption of block copolymers by rather weak hydrophobic interactions,⁴³ P4VP₂₅-*b*-PS(I)₃₅₀ grafted films were found to be very stable in various solvents even under ultrasonic bath conditions.

A dry thickness of the grafted P4VP₂₅-*b*-PS(I)₃₅₀ films equal to $h_{\text{P4VP-}b\text{-PS(I)}}$ \approx 8 nm is typical for polymer monolayers obtained by the “grafting-to” approach.⁴⁴ From the volume fraction of the P4VP block, the thickness of the anchoring P4VP layer is estimated to be \sim 0.5 nm. The thickness of the PS(I)₃₅₀ block of about 7.5 nm corresponds to a distance between adjacent chains, $D \approx$ 2.9 nm (Scheme 3) and a grafting density, $\sigma \approx$ 0.11 chains/nm².⁴¹ Assuming the radii of gyration, R_g , for PS(I)₃₅₀ in toluene to be approximately the same as for PS₃₅₀,⁴⁵ the reduced tethered density (Σ) was estimated to be $\Sigma = \sigma\pi R_g^2 \approx$ 12.4. The values of Σ and σ show that grafted P4VP₂₅-*b*-PS(I)₃₅₀ chains are in a “true brush” regime, however, not too far from the “mushroom-to-brush” transition.⁴³ The P4VP₂₅-*b*-PS(I)₃₅₀ brushes show good swellability in good solvents; for example, the thickness of the P4VP₂₅-*b*-PS(I)₃₅₀ brush in THF was found to be \sim 15 nm, as determined by in situ ellipsometry.

We demonstrated previously that the swellability of the PS(Br) networks, allowing the penetration of the Ni(PPh₃)₄ catalyst and the monomer is an important prerequisite for successful grafting of P3HT. We also found that the grafting of P3HT occurs not only from reactive sites developed in the topmost PS(Br) layer, but that very inner layers also contribute to the grafting process resulting into a kind of PS(I)-*graft*-P3HT network in which relatively short P3HT grafts emanate from PS(Br) strands, whereas the polymerization from PS(Br) monolayers is much less efficient. Translating this knowledge to the P4VP₂₅-*b*-PS(I)₃₅₀ brush system we expected that the grafting of P3HT will proceed from many sites developed along tethered PS(I) chains converting the “normal” planar P4VP-*b*-PS(I)-brushes into brushes of a P4VP-*b*-PS(I)-*graft*-P3HT graft copolymer (Scheme 3).

Activation of 8 nm-thick P4VP₂₅-*b*-PS(I)₃₅₀ brushes with Ni(PPh₃)₄ catalyst and subsequent placement of the activated brushes into the monomer solution leads to selective polycondensation of the monomer from the surface according to Scheme 1. The composite P4VP-*b*-PS(I)-*graft*-P3HT films show rela-

tively smooth morphology (rms roughness \approx 1 nm, Figure 1 b); the maximal achievable thickness lies between 30 and 50 nm. One, however, should keep in mind that in a reality the structure of the resulting surface-grafted P4VP-*b*-PS(I)-*graft*-P3HT chains might deviate from the idealized “tree-like” structure proposed in Scheme 3 because of undesired cross-linking reactions possibly occurring during the stage of the catalyst immobilization and further grafting of P3HT. Although Ni(PPh₃)₄ is widely used in cross-coupling reactions, homocoupling is a frequent undesired reaction: $\text{Ar-I} + \text{Ni}(\text{PPh}_3)_4 \rightarrow \text{Ar-Ni}(\text{PPh}_3)_2\text{-I}$; $2\text{Ar-Ni}(\text{PPh}_3)_2\text{-I} \rightarrow \text{Ar-Ar}$. This problem would be especially critical for multifunctional macromolecular compounds having a plurality of Ar-Ni-(PPh₃)₂-X moieties since in this case even vanishing yields of the homocoupling reaction can cause an extensive cross-linking. In order to evaluate the cross-linking process, model 8-nm-thick P4VP₂₅-*b*-PS(I)₃₅₀ brushes were treated with excess of Ni(PPh₃)₄ and quenched with acid water and their swelling behavior in THF was studied. We expected a decrease in the swellability if the cross-linking proceeds to a significant extent. However, just an opposite effect was found out. Although no iodine atom was detected by XPS investigation in such-treated P4VP₂₅-*b*-PS(I)₃₅₀ brushes suggesting a high yield of the catalyst immobilization, the swellability of the treated brushes in THF was distinctly and reproducibly higher than the swellability for the parent, untreated P4VP₂₅-*b*-PS(I)₃₅₀. This result excludes an extensive cross-linking during the catalyst immobilization, since in that case the swellability should be strongly suppressed. However, it might corroborate with the formation of lightly cross-linked P4VP₂₅-*b*-PS(I)₃₅₀ networks, which exhibit slightly higher swellability in THF, likely due to lower polarizability of iodine-free polystyrene units.

The above-described experiments, however, do not allow quantitative estimation of the cross-linking process. We suggested that a direct analysis of a polymeric material detached from the surface would shed more light onto the catalyst immobilization process. However, the absolute amount of materials that can adsorb onto planar surfaces is vanishing and this would require experiments with too large-area wafers. Therefore, silica gel particles with a large surface-to-volume ratio were used as a support. Micrometer-scale silica particles with low surface curvature rather than nanoscale silica particles were utilized in these experiments for an adequate modeling of the planar brush regime, as this factor can affect interchain interactions. A series of samples with a constant amount of adsorbed P4VP₂₅-*b*-PS(I)₃₅₀ was prepared and treated with Ni(PPh₃)₄ at varied Ni(PPh₃)₄-to-iodostyrene, [Ni]/S(I), ratio. The resulting polymer was afterward detached from silica gel by extraction with pyridine and analyzed by GPC. It was found that the treatment of P4VP₂₅-*b*-PS(I)₃₅₀ with amounts of Ni(PPh₃)₄ close to equimolar results into insoluble materials. Furthermore, because of low solubility, the GPC analysis was impossible to perform for the samples with [Ni]/S(I) ratios higher than 1:10. On the other hand, GPC traces of P4VP₂₅-*b*-PS(I)₃₅₀ treated at less than 1:50 [Ni]/S(I) ratios were found to be virtually indistinguishable from the GPC trace of the starting polymer. This suggests the absence of the intermolecular cross-linking in this regime, although the formation of some intramolecular links could not be excluded. An onset of the cross-linking process occurs at an \sim 1:33 [Ni]/S(I) ratio, as seen from the appearance on the GPC trace of a shoulder peaking at, approximately, doubled, compared to the starting P4VP₂₅-*b*-PS(I)₃₅₀, molecular weight (Figure S2, Supporting Information).

(43) Kent, M. S. *Macromol. Rapid Commun.* **2000**, *21*, 243–70.

(44) Brittain, W. J.; Minko, S. *J. Polym. Sci., Part A: Polym. Chem.* **2007**, *45*, 3505–12.

(45) (a) The radius of gyration (R_g) for free PS coils in toluene can be estimated as follows. $R_g = 0.117\text{MW}^{0.595}$; $R_g \approx$ 6 nm for PS with MW = 36 700 Higo, Y.; Ueno, N.; Noda, I. *Polym. J.* **1983**, *15*, 367–75. (b) Kent, M. S.; Lee, L.-T.; Farnoux, B.; Rondelez, F. *Macromolecules* **1992**, *25*, 6240–7.

Table 1. Thicknesses in the Dry and Swollen States, λ_{\max} and Estimated DPs for the P4VP-*b*-PS(I)-*g*-P3HT Composite Films and the Parent P4VP-*b*-PS(I) Brush

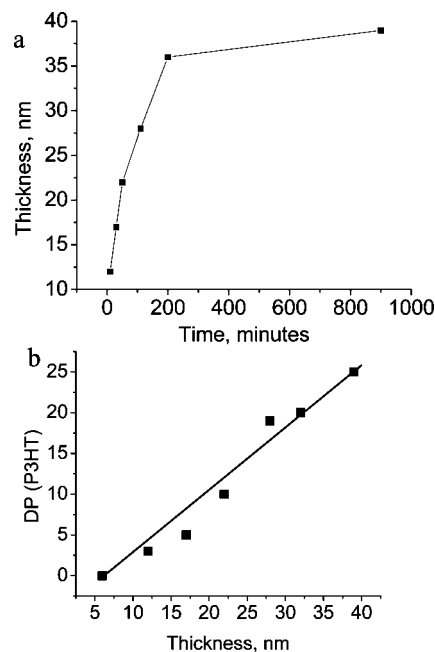
entry	T , min	λ_{\max} , nm	calculated DP of P3HT grafts	h_{dry} , nm	h_{THF} , nm
1	0	—	—	6	15
2 ^a	0	—	—	6	18 ^a
3	10	400	<5	12	26
4	30	420	~5	17	31
5	50	445	10	22	37
6	110	485	19	28	45
7	200	487	20	32	50
8	900	505	25	39	60

^a In this experiment the P4VP-*b*-PS(I) brush was converted into P4VP-*b*-PS by the treatment with Ni(PPh₃)₄ followed by the quenching with water.

The cross-linking process abruptly develops at higher [Ni]/S(I) ratios, so that a substantial fraction of insoluble materials is formed already at 1:20 [Ni]/S(I) ratio. Taking into account the amount of iodostyrene units per each P4VP₂₅-*b*-PS(I)₃₅₀ chain that participate in the reaction with Ni(PPh₃)₄ (350:33 = 10.6 and 350:20 = 17.5 for the 1:33 and 1:20 ratios, respectively) and assuming that the formation of, at least, one intermolecular link per each polymer chain is required for the dimerization (homocoupling), one can estimate the yield of the undesired homocoupling reaction. For the conditions used in our experiments it lies in the range from ~9% (100:10.6) to ~6% (100:17.5).

To monitor the grafting of P3HT in time, we prepared a series of 8 nm-thick P4VP₂₅-*b*-PS(I)₃₅₀ brush samples on Si wafers and glass slides, activated them with Ni(PPh₃)₄ catalyst and exposed them to the monomer solution for different times ranging from 10 to 900 min.⁴⁶ We found that the films continue to grow substantially within 3 h and further increase of the reaction time moderately increases their thickness. The results of the ellipsometric thickness measurements for the resulting composite P4VP-*b*-PS(I)-*graft*-P3HT films polymerized at different time at 0 °C are given in Table 1 and plotted in Figure 2a.

Unfortunately, a precise determination of the grafting density of P3HT along the PS(I) backbone and the polymerization degree (DP) of P3HT grafts to verify the postulated structure for the resulting film (Scheme 3) is a challenging task since it is impossible to detach selectively P3HT chains grown from PS(I). Furthermore, the analysis of the P4VP-*b*-PS(I)-*graft*-P3HT detached from the surface was failed because of its insolubility caused by homocoupling reactions (see above). However, a crude estimation of the molecular weight of the P3HT grafts can be made from UV-vis spectra. It is known that increase of the DP of regioregular head-to-tail P3HT results into gradual red-shift in the adsorption spectra,⁴⁷ especially in “bad” solvents and in the solid state.⁴⁸ To calibrate UV-vis absorption versus DP, we synthesized several P3HT samples of different DPs according to the previously reported method.³⁰ It was found, that increase of the DP from 5 to 30,⁴⁹ results in

**Figure 2.** Dry-state thickness of P4VP-*b*-PS(I)-*g*-P3HT films grown at different polymerization time (a) and development of the DP of the P3HT grafts (as estimated from UV-vis data) upon the P3HT grafting (b).

the red-shift of the main absorption band from $\lambda_{\max} = 420$ –518 nm (Figure S2).⁴¹

UV-vis spectra of grafted P3HT show that increase of the grafting time results in a gradual increase of the absorption intensity and in the red-shift of the position of the λ_{\max} from 420 to 505 nm that corresponds to the evolution of the DP from <5 to ~25 (Figures 3a and S3⁴¹).

The later value is consistent with the kinetic chain length determined previously for the “bulk solution” polycondensation of **1** mediated by the model (Ph)Ni(PPh₃)₂Br initiator under the same reaction conditions, as in the “grafting-from” experiments.³⁰ It is interesting to note that the DPs of the P3HT grafts grown at different polymerization time show a near straight-line dependence on the thickness of the P4VP-*b*-PS(I)-*graft*-P3HT (Figure 2b) suggesting the number of the polymerization sites to be constant (that corresponds to a fast initiating reaction).

From DP_{P3HT} and the observed film thickening upon the grafting of P3HT, the mean distance between the P3HT grafts along the PS(I) backbone (k) (Scheme 3) can be estimated as follows. If we assume that each PS(I) monomer unit derives the P3HT graft (this situation corresponds to the maximal possible grafting density with the distance between the grafts, $k = 0.25$ nm), the observed increase of the film thickness from 7.5 to 38.5 nm upon the grafting will correspond to DP_{P3HT-imaginary} ≈ 3.8 .⁵⁰ Since in reality the DP_{P3HT} for 39-nm-thick film is equal to ~25 (as estimated from UV-vis data), P3HT grafts grow approximately from every seventh PS(I) monomer unit (25:3.8 \approx 6.6) corresponding to $k \approx 1.6$ nm. Compared to combed brushes of

(46) A precise monitoring of the evolution of the film thickness during the grafting for the given sample was not possible since the set-up for in situ ellipsometric measurements is not compatible with rather demanding polymerization conditions (air- and water-sensitivity, low temperature). The reaction course, therefore, was monitored for series of samples by the termination of the grafting process after a respective time.

(47) Trznadel, M.; Pron, A.; Zagorska, M.; Chrzaszcz, R.; Pielichowski, J. *Macromolecules* **1998**, *31*, 5051–8.

(48) (a) Kiriy, N.; Jähne, E.; Adler, H.-J.; Schneider, M.; Kiriy, A.; Gorodyska, G.; Minko, S.; Jehnichen, D.; Simon, P.; Fokin, A. A.; Stamm, M. *Nano Lett.* **2003**, *3*, 707–712. (b) Kiriy, N.; Kiriy, A.; Bocharova, V.; Stamm, M.; Plötner, M.; Krebs, F. C.; Senkowska, I.; Adler, H. *Chem. Mater.* **2004**, *16*, 4757–4764.

(49) DP was determined by ¹H NMR.

(50) $DP_{\text{P3HT-imaginary}} = m_{\text{PS(I)}} \times \rho_{\text{P3HT}} \times (h_{\text{PS(I)-graft-P3HT}} - h_{\text{PS(I)}}) / m_{\text{P3HT}} \times \rho_{\text{PS(I)}} \times h_{\text{PS(I)}} = 232 \times 1.33 \times (38.5 - 7.5) / 168 \times 2.0 \times 7.5 \approx 3.8$.

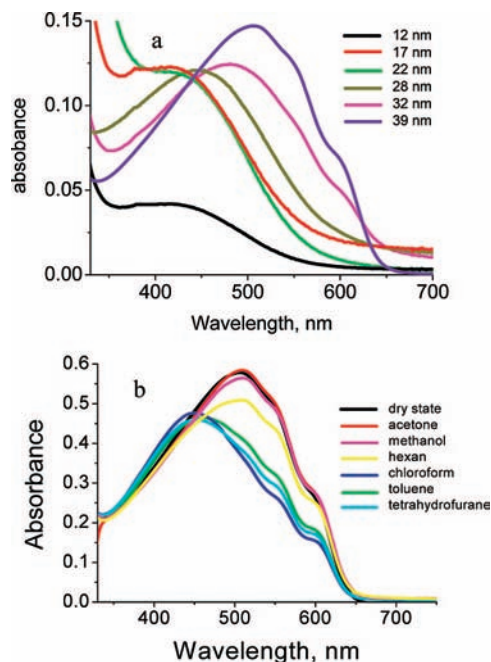


Figure 3. Development of UV-vis spectra of P4VP-*b*-PS(I)-*g*-P3HT brushes upon the grafting of P3HT (a); UV-vis spectra of P4VP-*b*-PS(I)-*g*-P3HT brushes in different solvents.

nonconjugated polymers reported by Matyjaszewski et al. for which polymer grafts propagate from each monomer unit of the main chain,⁵¹ the grafting density observed in our work is much less. Nevertheless, even such grafting density provides significant stretching of the main chain of the tethered graft copolymer, as demonstrated below.

The swelling behavior of the P4VP-*b*-PS(I)-*graft*-P3HT was studied by in situ ellipsometry and compared with the behavior of the parent P4VP-*b*-PS(I) brushes (Table 1). We found that the P4VP-*b*-PS(I)-*graft*-P3HT composite films swell to higher thicknesses than the parent P4VP-PS(I) brushes that might be attributed to increased excluded volume interactions of the graft copolymer (Table 1). The size of the PS(I) coil ($h_{\text{PS(I)-THF}}$ and $h_{\text{PS(I)-dry}}$ for the swollen layer in THF and in the dry state, respectively) can be evaluated subtracting from the overall film thickness ($h_{\text{PS(I)-THF}}$ or $h_{\text{PS(I)-dry}}$) the thickness of the anchoring P4VP layer (that is negligibly small, i.e., 0.5 nm, since P4VP chains are grafted to the surface by many points) and the contour length of the P3HT graft ($L_{\text{P3HT}} \approx 10$ nm for $D_{\text{P3HT}} = 25$, Scheme 3). Thus, $h_{\text{PS(I)-THF}}$ for the swollen P4VP-*b*-PS(I)-*graft*-P3HT film is equal to $60 - 0.5 - 10 \approx 50$ nm that is comparable with the PS(I) contour length ($350 \times 0.25 \approx 87$ nm). In the dry state the contribution from the P3HT grafts into the overall thickness is somewhat less due to the possible tilting and/or coiling of the P3HT chains and roughly equal to the thickness of the P3HT brushes obtainable from the PS(I) monolayers (~ 6 nm). Thus, $h_{\text{PS(I)-dry}}$ can be estimated at the level of $39 - 0.5 - 6 \approx 33$ nm. In both the dry and the swollen states the PS(I) backbone in P4VP-*b*-PS(I)-*graft*-P3HT is much more stretched than it is in the starting P4VP-*b*-PS(I) (7.5 and 14.5 nm for the dry and swollen states, respectively). Thus, the grafting from the polymer brushes leading to increase the side-chain bulkiness is an efficient way to increase of the stretching degree of the tethered polymer chains at constant grafting

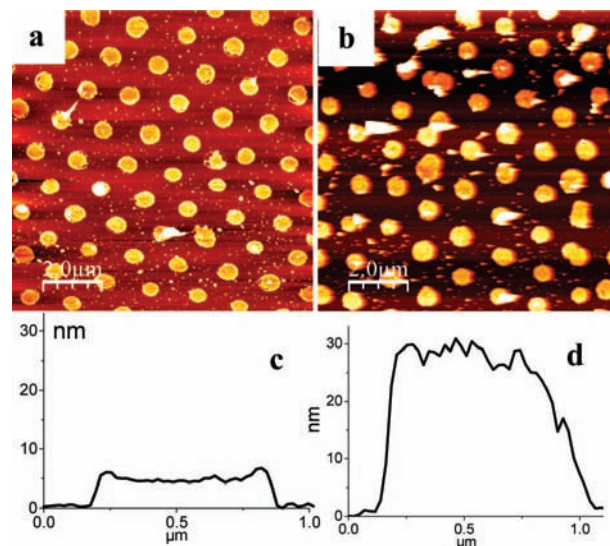


Figure 4. AFM topography images (a, b) and cross-sections (c, d) of micropatterned P4VP₂₅-*b*-PS(I)₃₅₀ (a, c) and P4VP₂₅-*b*-PS(I)₃₅₀-*g*-P3HT (b, d) brushes.

density. Such a behavior for strongly overlapping comblike brushes was theoretically predicted by Zhulina and Vilgis.⁵²

UV-vis spectra of the grafted P3HT recorded in different solvents reveal their solvatochromism similar to one previously observed for dissolved P3HT (Figure 3b). It is, however, interesting to note, that although “good” solvents (THF, toluene, and CHCl₃) cause an important blue-shift of the λ_{max} , some shoulders at 500–600 nm are still remaining. This reflects a significant aggregation and/or planarization of tethered P3HT chains that occurs even in “good” solvents and might be due to decreased entropy of the grafted chains.

Micro- and nanoscale patterning of the P3HT brushes is an important step to exploit them in opto-electronic devices and sensors. Specific and strong adsorptivity of the P4VP block to polar metallic and metal oxide surfaces was utilized in this work to pattern P4VP₂₅-*b*-PS(I)₃₅₀. In principle, various kinds of lithography techniques (microcontact printing, photo-, dip-pen, and inject-printing lithography) can be applied for the site-specific deposition of the reactive block copolymer. As an example, in this work we used a kind of colloidal lithography⁵³ according to which sub-micrometer hydrogel particles were arranged on Si wafers by dip coating and used as a mask (Scheme 2). Afterward, the samples were treated by ODS to deactivate (hydrophobize) the space between the particles. After the removal of the particles P4VP₂₅-*b*-PS(I)₃₅₀ was adsorbed selectively onto remaining hydrophilic spots. AFM reveals the successful microstructuring of P4VP₂₅-*b*-PS(I)₃₅₀ into quasi-periodic hexagonal array of round-shaped disks of 8 nm in height and ~ 1 μm in diameter (Figure 4c). Subsequent treatment of the samples with Ni catalyst and monomer solution results in selective grafting of P3HT from the patterned P4VP₂₅-*b*-PS(I)₃₅₀ disks, as evidenced by increase of their thickness up to 30 nm (Figure 4d).

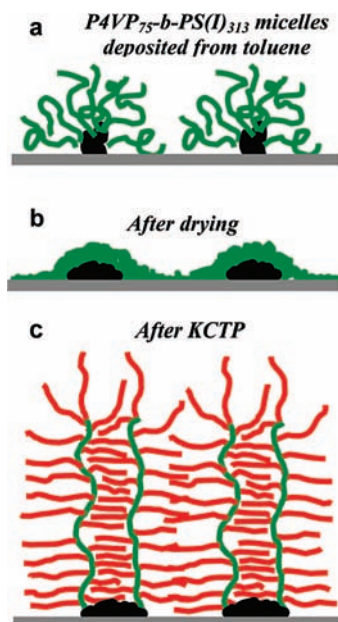
It is well-known that well-defined block copolymers provide interesting possibilities for nanopatterning.^{32,54} P4VP₂₅-*b*-PS(I)₃₅₀ does not form micelles in solvents selective for PS(I) since the P4VP block is too small. Therefore, the less asymmetric P4VP₇₅-

(51) Borner, H. G.; Beers, K.; Matyjaszewski, K.; Sheiko, S. S.; Moller, M. *Macromolecules* **2001**, *34*, 4375–4383.

(52) Zhulina, E. B.; Vilgis, T. A. *Macromolecules* **1995**, *28*, 1008–15.

(53) Henzie, J.; Barton, J. E.; Stender, C. L.; Odom, T. W. *Acc. Chem. Res.* **2006**, *39*, 249–57.

Scheme 4. Schematic Representation of the Formation of Nanostructured P4VP-*b*-PS(I)-*g*-P3HT Brushes



b-PS(I)₃₁₃ was used for the nanostructuring. A micellar dispersion of P4VP₇₅-*b*-PS(I)₃₁₃ in toluene was spin-coated onto Si wafers and samples were annealed at 150 °C in inert atmosphere.

At this temperature, PS(I) constituting the shell of the micelles does not melt and acts as nanoreactor in which molten P4VP chains will be grafted to the surface (Scheme 4). As a result, the P4VP₇₅-*b*-PS(I)₃₁₃ monolayer preserves the characteristic quasi-regular arrangement of micelles even after extensive rinsing with solvents good for both blocks (THF and chloroform). AFM reveals nanostructures with a height of undulations of ~6 nm and mean distance between centers of micelles of ~45 nm (Figure 5a,b and Scheme 4). Previously, the formation of nanophase separated structures given by the incompatibility of the polymer components was reported for binary brushes with surface pattern sensitive to the kind of the solvent applied. In contrast, the method presented in this paper gives nanostructured brushes with the pattern independent of the solvent pretreatment since the chains were firmly tethered in the segregated state. Subsequent activation of the 6-nm-thick nanostructured brushes with the Ni(PPh₃)₄ catalyst and placement of them into the monomer solution results in grafting of P3HT. This is evident from the substantial increase of the initial brush thickness (see cross-sections Figure 5c vs f). Although, the grafting of P3HT destroys the initial order, the particulate morphology in the resulting film is preserved (Figure 5d).

Photovoltaic Properties. It is believed that performance of solar cells can be further improved through a proper organization of the nanoscale morphology of bulk heterojunctions.⁵⁵ It was theoretically predicted that in “ideal” bulk heterojunctions the first component (e.g., electron-donating P3HT) must be featured into nanoscale columns penetrating the matrix of the second component (e.g., electron-accepting fullerene). It is essential that

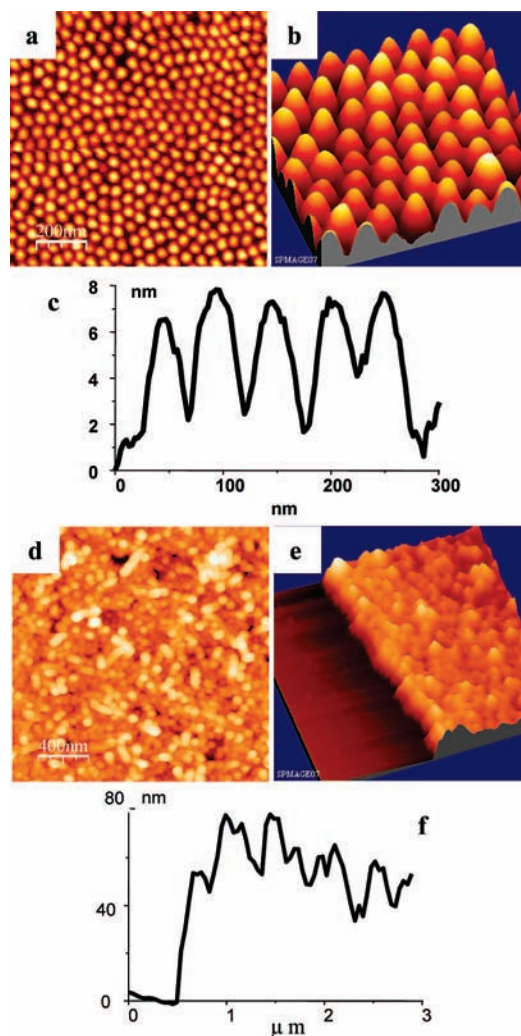


Figure 5. AFM images (a, b, d, e) and cross-sections (c, f) of the nanostructured P4VP₇₅-*b*-PS(I)₃₁₃ and P4VP₇₅-*b*-PS(I)₃₁₃-*g*-P3HT brushes.

all polymer chains constituting the columns should be directly connected to the anode and aligned along the main axis of the columns, thus forming an optimized conditions for a charge-separation and providing dead-end-free pathways for charges.⁵⁶ Keeping this in mind, the method to grow P3HT brushes with P3HT main chains directly attached to the anode is strongly desired. In this work P4VP-PS-*g*-P3HT brush was either grown from a PEDOT layer or directly from ITO. However, all samples showed low photovoltaic characteristics (Figures S4 and S5, Supporting Information). Typically, the samples showed a very small short circuit current density J_{sc} up to ~0.2 mA/cm², a small open circuit voltage V_{oc} up to 0.2 V, a small fill factor FF of 26% and the overall power conversion efficiency not more than 0.01%. The large bias dependency of the photocurrent is a sign for problems in exciton separation and charge carrier transport. P4VP-*b*-PS(I)-*graft*-P3HT brushes displayed only poor photovoltaic properties, most likely due to their structure improper for charge carrier transport. There is an, at least, 0.5-nm-thick insulating P4VP layer at the interface between the brush and ITO and the orientation of the P3HT grafts is parallel to the interface (see Scheme 2). Additionally, the low molecular weight

(54) (a) Ruokolainen, J.; Mäkinen, R.; Torkkeli, M.; Mäkelä, T.; Serimaa, R.; ten Birke, G.; Ikkala, O. *Science* **1998**, *280*, 557–60. (b) Sidorenko, A.; Tokarev, I.; Minko, S.; Stamm, M. *J. Am. Chem. Soc.* **2003**, *125*, 12211–6. (c) Kim, D. H.; Kim, S. H.; Lavery, K.; Russell, T. P. *Nano Lett.* **2004**, *4*, 1841–4.

(55) Kannan, B.; Castellino, K.; Majumdar, A. *Nano Lett.* **2003**, *3*, 1729–33.

(56) Snaith, H. J.; Whiting, G. L.; Sun, B.; Greenham, N. C.; Huck, W. T. S.; Friend, R. H. *Nano Lett.* **2005**, *5*, 1653–7.

of P3HT grafts limits the charge carrier mobility.⁵⁸ An absence of the photovoltaic response for the sample in which P4VP-PS(I)-*g*-P3HT was developed on PEDOT–PSS interlayer likely originates from the reductive nature of the polymerization mixture containing the Grignard reagent possibly caused dedoping of the PEDOT transforming it into a poor conductor. Unfortunately, grafting from a (EtO)₃Si–Ph(Br) silane monolayer, which would provide a minimal separation between tethered P3HT and conducting support lead to a marginal deposition of P3HT because of termination processes. Thus, further optimizations of the grafting procedure are needed which is currently under way in our laboratory.

On the other hand, the polymer structures developed herein would be attractive materials for manufacturing of regenerable sensors in which surface-tethered conjugated polymers with conformation-dependent properties will act as transducers converting (bio)chemical signals into optical ones. Preliminary investigations demonstrate that the surface-initiated KCTP could be extended onto other, more functional kinds of monomers (i.e., 2-bromo-5-chloromagnesio-3-bromohexylthiophene) leading to surface-tethered poly[3-(6-bromohexyl)thiophene], P3BrHT, easily convertible onto a variety of conjugated polyelectrolytes. Postpolymerization modifications of P3BrHT developed by McCullough et al.⁵⁹ work well also for grafted P3BrHT leading to highly water-swallowable conjugated polyelectrolyte brushes.⁶⁰ We believe that utilization of surface-immobilized patterned conjugated polymers for biosensing would have technological advantages compared to sensors used dissolved conductive polymers.^{21,61}

Conclusions

P4VP-*b*-PS(I) block copolymers obtained by the iodination of readily available P4VP-*b*-PS block copolymers strongly adsorb to a variety of polar substrates including Si-wafers, glasses and metal oxide surfaces due to polarity of the P4VP block forming moderately stretched PS(I) brushes. Kumada

catalyst transfer polycondensation from the P4VP-*b*-PS(I) brushes preactivation with the Ni(PPh₃)₄ catalyst results into planar brushes of the graft copolymer with the relatively short (~10 nm) P3HT grafts emanating from the surface-tethered PS(I) chains. Grafting of the P3HT leads to significant stretching of the PS(I) backbone as a result of increased excluded volume interaction. Although a number of comblike polymers was synthesized to date,⁵¹ including a graft copolymer with the P3HT side chains,⁶² examples of end-tethered graft copolymers remain scarce.⁶³ Furthermore, the P4VP-PS(I)-*g*-P3HT brush reported herein is the first, to the best of our knowledge, example of an end-tethered conjugated graft copolymers reported to date. Specific adsorption of the P4VP block to polar surfaces was utilized in this work to pattern P4VP₂₅-*b*-PS(I)₃₅₀ brush. The microscopically structured P4VP₂₅-*b*-PS(I)₃₅₀ brush was converted into the respectively patterned P4VP-PS(I)-*g*-P3HT one. We demonstrated that the functional block copolymers are also an attractive option for nanostructuring of polymer brushes. P4VP₇₅-*b*-PS(I)₃₁₃ micelles obtained in a selective solvent for the PS(I) block form quasi-ordered hexagonal arrays on Si-wafer. The PS(I) shell due to the high glass transition point of PS(I) (200 °C) prevents the diffusion of the P4VP anchoring block over the whole surface and therefore the order is remained even after the grafting at 150 °C. The P4VP₇₅-*b*-PS(I)₃₁₃ brushes preserve the characteristic quasi-regular arrangement of the micelles even after the extensive rinsing with various solvents. P4VP-*b*-PS(I)-*graft*-P3HT brushes display poor photovoltaic properties, most likely due to their structure improper for the charge-separation. Nevertheless, we believe that the method of the site-specific polycondensation into structured brushes of conductive polymers reported herein will be a helpful tool for engineering of novel stimuli-responsive materials, sensors, optoelectronic devices, photonic crystals, etc.

Acknowledgment. We thank Bettina Pilch and Ulrich Oertel for the UV measurements and a reviewer for valuable suggestions regarding cross-linking reactions. Financial support was provided by the Deutsche Forschungsgemeinschaft (STA 324/25-1, SFB 287/B1, and STA 324/32-1 (SPP 1259/1 “Intelligente Hydrogele”).

Supporting Information Available: ¹H NMR of P4VP-PS(I), GPC traces of degrafted polymers, and UV–vis spectra of different molecular weight P3HT samples. This material is available free of charge via the Internet at <http://pubs.acs.org>.

JA8050734

- (57) Brown, P. J.; Thomas, D. S.; Kohler, A.; Wilson, J. S.; Kim, J. S.; Ramsdale, C. M.; Siringhaus, H.; Friend, R. H. *Phys. Rev. B* **2003**, *67*, 064203.
- (58) Zhang, R.; Li, B.; Iovu, M. C.; Jeffries-EL, M.; Sauve, G.; Cooper, J.; Jia, S.; Tristram-Nagle, S.; Smilgies, D. M.; Lambeth, D. N.; McCullough, R. D.; Kowalewski, T. *J. Am. Chem. Soc.* **2006**, *128*, 3480–1.
- (59) (a) Zhai, L.; Pilston, R. L.; Zaiger, K. L.; Stokes, K. K.; McCullough, R. D. *Macromolecules* **2003**, *36*, 61–64. (b) Stokes, K. K.; Heuze, K.; McCullough, R. D. *Macromolecules* **2003**, *36*, 7114–18.
- (60) Preparation and characterization of conjugated polyelectrolyte brushes will be published elsewhere.
- (61) Nilsson, K. P. R.; Herland, A.; Hammarstrom, P.; Inganas, O. *Biochemistry* **2005**, *44*, 3718–24.

(62) Sivula, K.; Ball, Z. T.; Watanabe, N.; Frechet, J. M. J. *Adv. Mater.* **2006**, *18*, 206–10.

(63) Zhai, G.; Cao, Y.; Gao, J. *J. Appl. Polym. Sci.* **2006**, *102*, 2590–9.